COO-2245-25

COOLANT MIXING IN LMFBR ROD BUNDLES AND OUTLET PLENUM MIXING TRANSIENTS

Progress Report

Principal Investigators
Neil E. Todreas
Michael W. Golay

Massachusetts Institute of Technology
Department of Nuclear Engineering
Cambridge, Massachusetts 02139

June 1, 1975 - August 31, 1975

Prepared for the U.S. Energy Research and Development Administration under Contract No. AT(11-1)-2245

DISCLAIMER

Reports Issued Under This Contract

A. Quarterly Progress Reports

COO-2245-1 Period June 1, 1972 - November 30, 1972

COO-2245-2 Period December 1, 1972 - February 28, 1973

COO-2245-3 Period March 1, 1973 - May 31, 1973

COO-2245-6 Period June 1, 1973 - August 31, 1973

COO-2245-7 Period September 1, 1973 - November 30, 1973

COO-2245-8 Period December 1, 1973 - February 28, 1974

COO-2245-10 Period March 1, 1974 - May 31, 1974

COO-2245-13 Period June 1, 1974 - August 31, 1974

COO-2245-14 Period September 1, 1974 - November 31, 1974

COO-2245-15 Period December 1, 1974 - February 28, 1975

COO-2245-23 Period March 1, 1975 - May 31, 1975

COO-2245-25 Period June 1, 1975 - August 31, 1975

Reports Issued Under This Contract

B. Topical Reports

E. Khan and N. Todreas, "A Review of Recent Analytical and Experimental Studies Applicable to LMFBR Fuel and Blanket Assembly Design," COO-2245-4TR, MIT, Sept. 1973.

E. Khan, W. Rohsenow, A. Sonin and N. Todreas, "A Simplified Approach for Predicting Temperature Distribution in Wire Wrapped Assemblies," COO-2245-5TR, MIT, September 1973.

T. Eaton and N. Todreas, "Instrumentation Methods for Interchannel Coolant Mixing Studies in Wire-Wrap Spaced Nuclear Fuel Assemblies," COO-2245-9TR, MIT, June 1974.

Y. B. Chen, K. Ip, N. E. Todreas, "Velocity Measurements in Edge Subchannels of Wire Wrapped LMFBR Fuel Assemblies," COO-2245-11TR, MIT, September 1974.

E. Khan, N. Todreas, W. Rohsenow, A.A. Sonin, "Analysis of Mixing Data Relevant to Wire-Wrapped Fuel Assembly Thermal-Hydraulic Design," COO-2245-12TR, MIT, Sept. 1974.

E. Khan, W. Rohsenow, A. Sonin, N. Todreas, "A Porous Body Model for Predicting Temperature Distributions in Wire Wrapped Fuel and Blanket Assemblies of a LMFBR," COO-2245-16TR, MIT, March 1975.

E. Khan, W. M. Rohsenow, A. Sonin, N. Todreas, "Input Parameters to the ENERGY Code (To be used with the ENERGY Code Manual) COO-2245-17TR, MIT, May, 1975.

E. Khan, W. Rohsenow, A. Sonin, N. Todreas, "Manual for ENERGY Codes I, II, III," COO-2245-18TR, MIT, May 1975.

P. Carajilescov and N. Todreas, "Experimental and Analytical Study of Axial Turbulent Flows in an Interior Subchannel of a Bare Rod Bundle," COO-2245-19TR.

B. Chen and N. Todreas, "Prediction of Coolant Temperature Field in a Breeder Reactor Including Interassembly Heat Transfer," COO-2245-20TR, MIT, May 1975.

F. Carre and N. Todreas, "Development of Input Data to Energy Code for Analysis of Reactor Fuel Bundles," COO-2245-21TR, MIT, May, 1975.

Reports Issued Under This Contract

B. Topical Reports, Continued

H. Ninokata and N. E. Todreas, "Turbulent Momentum Exchange Coefficients for Reactor Fuel Bundle Analysis," COO-2245-22TR, MIT, June 1975.

R. Anoba and N. Todreas, "Coolant Mixing in LMFBR Rod Bundles and Outlet Plenum Mixing Transients," COO-2245-24TR, MIT, August, 1975

Reports Issued Under This Contract

C. Papers and Summaries

Yi Bin Chen, Ka-Lam Ip, Neil E. Todreas, "Velocity Measurements in Edge Channels of Wire-Wrapped LMFBR Fuel Assemblies," American Nuclear Society Transactions. Vol. 19, 1974, pp. 323-324.

P. Carajilescov, N. Todreas, "Experimental and Analytical Study of Axial Turbulent Flows in an Interior Subchannel of a Bare Rod Bundle," accepted for the ASME Winter Annual Meeting, Nov. 1975 (Included as Appendix to Quarterly Progress Report COO-2245-15).

E. Khan, W. Rohsenow, A. Sonin, N. Todreas, "A Porous Body Model for Predicting Temperature Distribution in Wire-Wrapped Fuel Rod Assemblies," Submitted to Nuclear Engineering and Design.

B. Chen and N. Todreas, "Prediction of Coolant Temperature Field in a Breeder Reactor Including Interassembly Heat Transfer," Submitted to Nuclear Engineering and Design (included as Appendix to Quarterly Progress Report COO-2245-23).

E. Khan, W. Rohsenow, A. Sonin, N. Todreas, "A Porous Body Model for Predicting Temperature Distribution in Wire-Wrapped Rod Assemblies Operating in Combined Forced and Free Convection, Submitted to Nuclear Engineering and Design.

COOLANT MIXING IN LMFBR ROD BUNDLES AND OUTLET PLENUM MIXING TRANSIENTS

Contract AT(11-1)-2245

Quarterly Progress Report

June 1, 1975 - August 31, 1975

The work of this contract has been divided into the following Tasks:

TASK I: BUNDLE GEOMETRY (WRAPPED AND BARE RODS)

- TASK IA: Assessment of Available Data
- TASK IB: Experimental Bundle Water Mixing Investigation
- TASK IC: Experimental Bundle Peripheral Velocity Measurements (Laser Anemometer)
- TASK ID: Analytic Model Development - Bundles

TASK II: SUBCHANNEL GEOMETRY (BARE RODS)

- TASK IIA: Assessment of Available Data
- TASK IIB: Experimental Subchannel Water Mixing Investigation
- TASK IIC: Experimental Subchannel Local Parameter Measurements (Laser Anemometer)
- TASK IID: Analytic Model Development - Subchannels

TASK III: LMFBR OUTLET PLENUM FLOW MIXING

- TASK IIIA: Analytical and Experimental Investigation of Velocity and Temperature Fields

TASK I: BUNDLE GEOMETRY (WRAPPED AND BARE RODS)

TASK IA: Assessment of Available Data

No work was performed this quarter.

TASK IB: Experimental Bundle Water Mixing Investigation

1) 61-Pin Fuel Experiments (Alan Hanson)

Following the completion of mixing experiments with the 6-inch wire-wrap lead fuel bundle during the previous quarter, the test section was disassembled, cleaned and then reassembled with a new set of 12-inch wire wrap lead fuel pins. Three tracer injection rods were included in this bundle instead of the two used in previous experiments. The injector rod locations are shown in Figure 1; the new injector is the one located one row in from the front edge of the bundle.

During the bundle changeover period, a major change was made to the injection system. Examination of the old galvanized salt holding tank revealed some corrosion and salt deposition in the bottom of the tank. Since any reaction which removes sodium or chloride ions from the injection solution would tend to lower the apparent injection concentration, this could be part of the difficulty in obtaining good mass balances. Therefore the 30-gallon galvanized tank was replaced by a 60-gallon stainless steel tank that was available.

The main accomplishment of this quarter was the collection of a set of mixing data from the 12-inch bundle analogous to that taken from the 6-inch bundle. Three experimental runs were made with each of the three injector rods. Details of these runs are listed in Table 1. The first two runs were made to illustrate the axial development of the salt distributions in turbulent and laminar flow regimes, and the third run was planned to check for any effects of Reynolds number on the salt mixing. Most of the data from these experiments have been reduced and are currently being compared with those taken previously on the 6-inch bundle. It appears that despite the new stainless steel injection tank, mass balances have not improved. Although mass balances for the turbulent runs in the 12-inch bundle are slightly better than corresponding 6-inch bundle data, the mass balances for laminar runs in the 12-inch bundle are significantly worse than in the 6-inch bundle cases. The inability to obtain good laminar flow data is not too surprising because of expected streamlining effects and

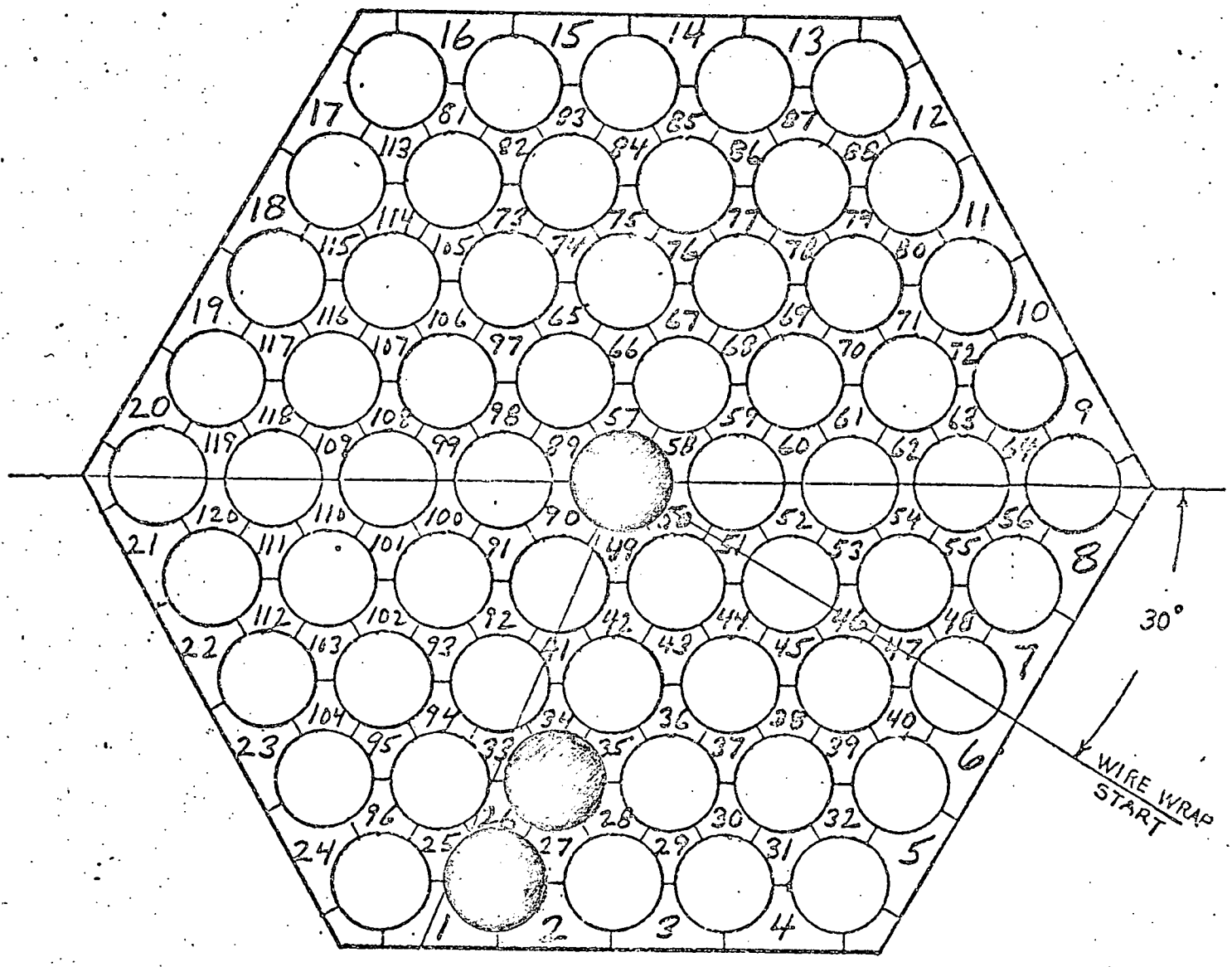

FIGURE 1 CROSS SECTIONAL SKETCH OF TEST SECTION

TABLE I

MIXING EXPERIMENT PARAMETERS FOR 12"-LEAD BUNDLE

Run	Flowrate	Reynolds Number	Flow Regime	Injector Arial Location	Injection Concentration
1	55	8140	Turbulent	1" - 26" *	3.8%
2	5	740	Laminar	1" - 26" *	3.8%
3	2.5 - 100 **	370 - 14,800	Laminar-Turbulent	23"	3.8%

* Data taken at 38 different axial locations

** Data taken at 10 different flowrates

the lack of turbulent exchange to break up the stream-lines. Qualitatively, a comparison of 12-inch bundle data with 6-inch bundle results shows that less mixing is occurring in the 12-inch bundle and the survival flow is also less in the 12-inch bundle.

In addition to the mixing data, pressure measurements were made on the 12-inch bundle. Detailed axial pressure traverses using the injector rods were taken and showed the same periodicity with wire-wrap lead length that was previously observed in the 12-inch bundle. However, the magnitude of the static pressure variations both axially and transversely were much less in the 12-inch bundle than in the 6-inch bundle.

A complete analysis of all data taken from the 12-inch wire-wrap lead bundle is planned for the next quarter. Included will be a comparison of the data with predictions using the ENERGY Code.

TASK IB: Experimental Bundle Water Mixing Investigation

(Brian Bosy)

2) A second set of face plates and peripheral rods was prepared this quarter to permit testing of half size wire wrap on the edge rods.

TASK IC: Experimental Bundle Peripheral Velocity Measurements (Laser Anemometer)

(R. Anoba and C. Chong)

During this quarter work has been done on attempting to collect data of the edge channel velocity measurements in wire wrapped LMFBR prototype blanket 61-pin bundle. Due to difficulties encountered, velocity data was not obtained by using the Laser Doppler Anemometer method.

The following difficulties were encountered:

1) Two Phase Flow Oscillations

The pre-operational testing of the flow loop indicated unstable fluctuations in the flow meter reading along with oscillations of the water level in the upper plenum. This phenomenon is believed to be caused by air entering the discharge line due to the low pressure at the bundle exit. This two phase oscillation was successfully suppressed by shortening the discharge line and collecting the exiting fluid in an intermediate tank prior to its final discharge.

2) Highly Amplitude Modulated Noise

In this experiment, noise was tracked in all frequency ranges of the signal processor when the laser equipment was activated. After the noise was partly suppressed by building a bandpass filter between the bus line and the electronic equipment, the highly amplitude modulated noise was still observed on the oscilloscope. Therefore, it was decided to switch to the two beams (one component) scheme so that reliable results could be acquired instead of attempting to achieve the initial goals by using four beams (two components) crossing on the measuring volume.

Furthermore, since the DISA Mark II system allows shifting of the doppler signals into 50 MHZ region, the S/N ratio could be considerably improved. This new system has been used in the later part of our experimental work. The alignment of this new system is shown in Figure 2.

This new LDA system has some improved features relative to our work. First, direct 180° focusing is possible which can increase our capacity of performing measurements deep into the bundle. Second, at zero velocity the shift can be used to generate a doppler signal with which the electronic equipment can be checked. On the other hand, because of the 180° focusing we also found that the peripheral velocity data was not available at some positions in which the back reflection light is strong.

Characteristics of Data Acquisition

With the DISA Mark II system, some weak but interpretable data were obtained. The experimental conditions under which this data was obtained are stated as follows:

1) Locations

The locations in which data were available and not available are shown in Figures 3 and 4.

2) Reynolds Numbers in Experiment

The data could only be obtained at a very low Reynolds number, i.e., Re = 84. Everytime we increased the Reynolds number, the doppler signals on the oscilliscope became indistinguishable on the background noise and they were not able to be tracked by the LDA system.

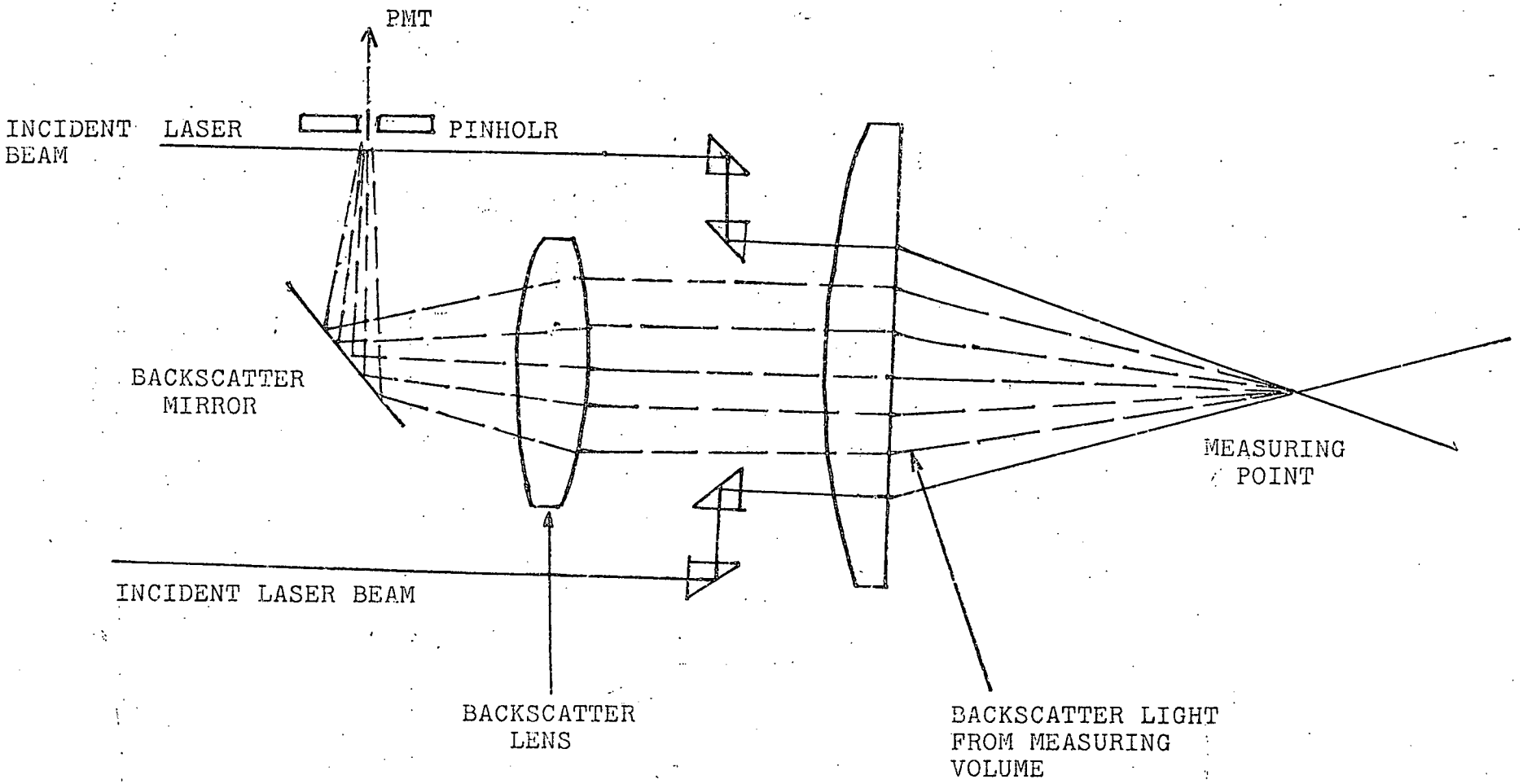

FIGURE 2

SCHEMATIC DIAGRAM OF DISA MARK II BACK-SCATTER MODE

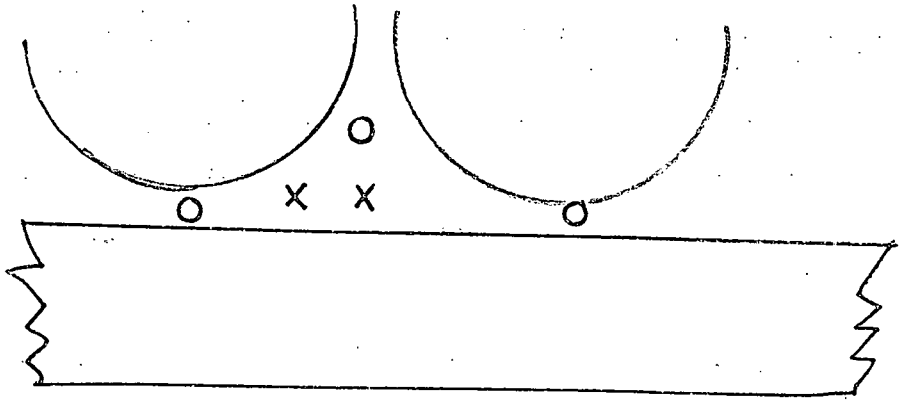

X --- DATA ARE OBTAINED IN THESE LOCATIONS

FIGURE 3
TOP VIEW OF LOCATIONS WHERE DATA ARE OBTAINED

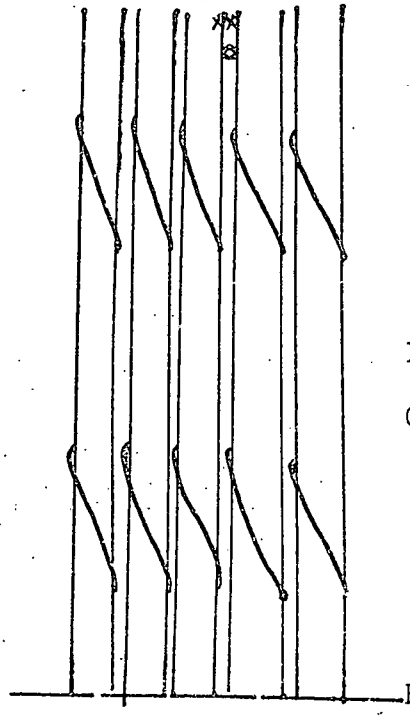

X = LOCATIONS WHERE DATA WAS OBTAINED

O = LOCATIONS WHERE DATA COULD NOT BE OBTAINED

FIGURE 4
FRONT VIEW OF LOCATIONS WHERE DATA ARE/ARE NOT OBTAINED

3) Components of the Peripheral Velocity Data

Interpretable data were obtained in axial component of the peripheral flow. Yet the data of 45 components could not be obtained. This problem was believed caused from lack of extensive check of the focus point of laser beams on the pin hole and therefore is not fundamental.

4) Characteristics of Signals

The Doppler signals shown on the oscilliscope were rather weak by comparison with the laminar signals obtained in other experiments. The difference is illustrated in Figure 5, below.

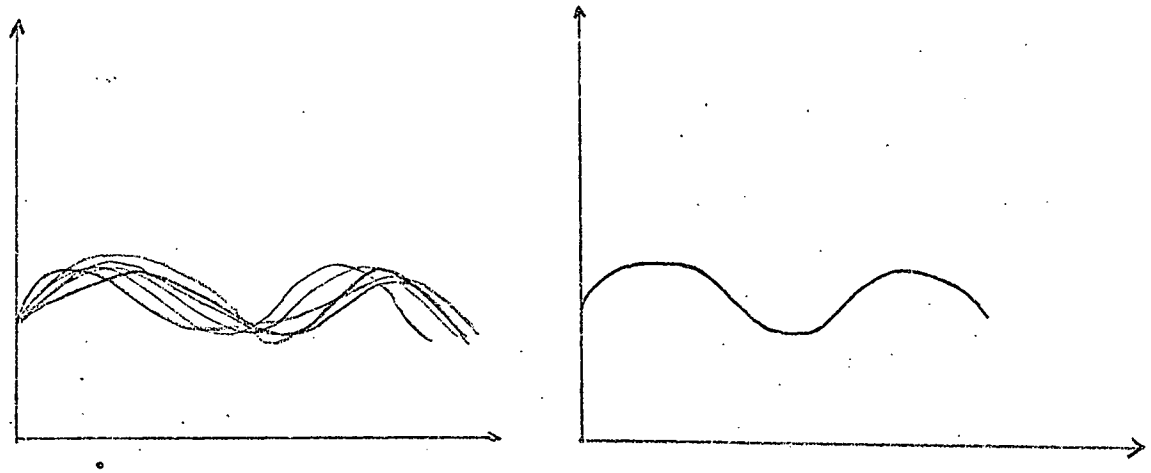

Figure 5

COMPARISON BETWEEN THE DOPPLER SIGNALS WE OBTAINED AND THOSE OBTAINED IN OTHER WORKS

5) Measuring Volumes

Two sizes of measuring volumes were used in this experiment. One has a major axis of 4.5 mm and a minor axis of 0.3 mm, the other has dimensions of 2.25 mm and 0.3 mm. Data could only be obtained within the smaller measuring volume (2.25 mm, 0.3 mm). This phenomenon is still not fully understood and it needs further study. The sizes of measuring volume used in this experiment compared with the size of the bundle is illustrated in Figure 6.

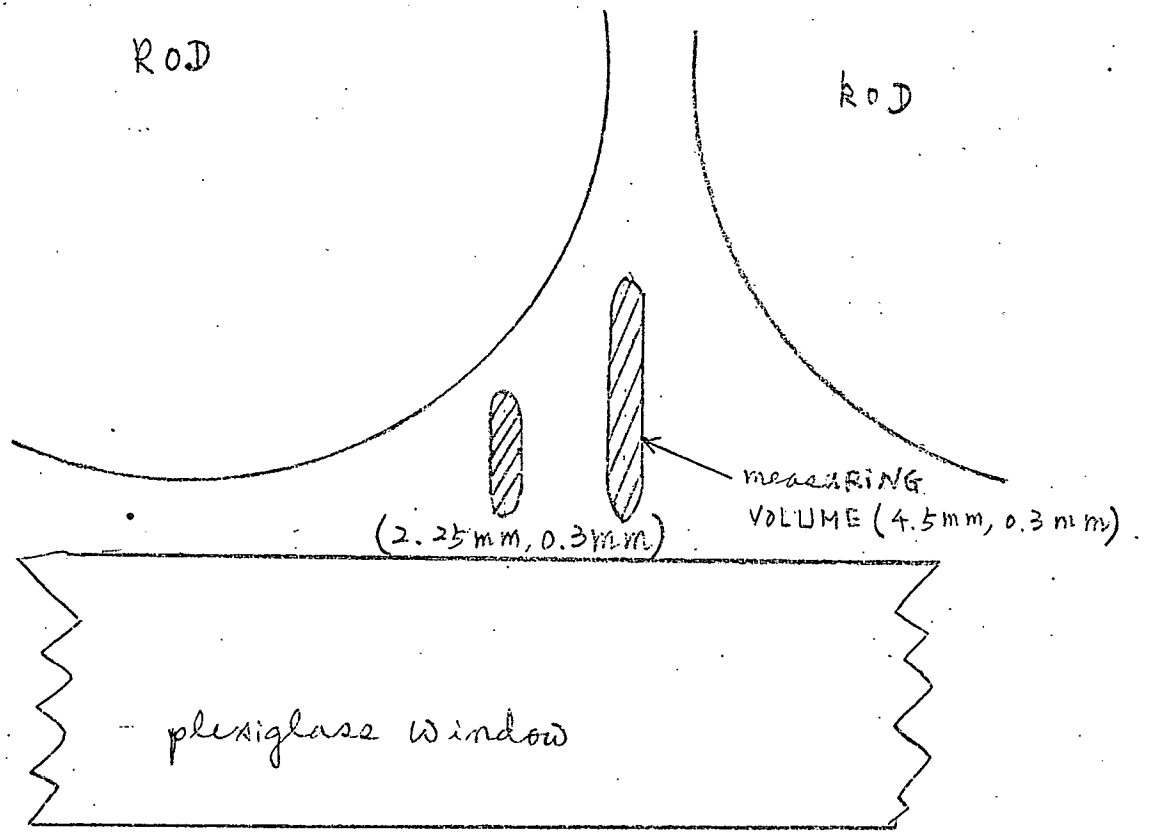

Fig 6. MEASURING VOLUME IN THE BUNDLE (TOP VIEW)

Possible Causes of Measurement Difficulties

The possible causes of the difficulties encountered are listed as follows:

1) The disturbance of the flow by support pins at the bottom of the test rods. However, since the measuring zone per figure 4 was over two lead lengths from the support pins, this possible cause does not appear to be responsible for the difficulties encountered.

2) Characteristics of the Flow

Since the lead length of wire wraps and the flow channel areas are smaller than those in the previous experiments, small eddies could probably be built up in the flow stream. If the scale of these eddies were smaller than the measuring volume, signal degradation could be due to turbulence broadening.

TASK ID: Analytical Methods Development

No work was performed this quarter.

TASK II: SUBCHANNEL GEOMETRY (BARE RODS)

TASK IIA: Assessment of Available Data

No new data published in the literature which could be assessed this quarter.

TASK IIB: Experimental Investigation (Joseph M. Kelly)

During the month of August, mixing tests were begun. The results of these showed that a diversion crossflow of a magnitude equal to about half the turbulent interchange existed in the test section. This development complicates our task in two ways.

In our experiment, we isokinetically sample the two central subchannels. The flowrates we extracted from the test section must be equal so that our sampling does not cause any additional crossflows. Since flowmeters are only accurate to 1-2% (the same order of magnitude as the mixing) and pressure measuring systems (for water, in the .01 inches of water range) are difficult to procure, we decided to use our fluorometer to balance the flows. If the test section can be assumed to be totally symmetrical, (an assumption often made in mixing experiments of this type) then by tracing first the right and then the left channels with the same dye concentration, the output of the receptor channels can be measured and should be identical. If a difference in output concentrations exist, then you assume the sampling technique is influencing the mixing and adjust the extracted flowrates until the concentration difference is nulled out.

However, in our tests, instead of making fine control adjustments, large adjustments had to be made and since the effect was repeatable and always in the same direction, we concluded that a diversion crossflow was built into our test section. Consequently, the basic tenet of the above discussion (perfect symmetry) was no longer valid and an alternate method of balancing the flows had to be found. In the past, we had searched for a good pressure sensor and had been unsuccessful, so we decided to design and construct one. The design appeared simple, two pressure cells separated by a diaphragm onto which strain gages were attached. Then by amplifying this voltage difference caused by a resistance change in the gages, pressures of .0001 psi could be measured, theoretically. However, difficulties occurring in the initial phases of construction coupled with the unexpected identification of a company that makes the needed type of pressure transducer, have lead us to purchase the commercially available system (Datometrics - Barocek "Electric Manometer"). The delivery dates for the unit is not yet established.

The second complexity arises in the data reduction technique. Originally we had a system of four differential equations of the type shown below:

$$\dot{m} \frac{dC_1}{dx} = W_I(C_2 - C_1) + 2W_{II} (C_3 - C_1)$$

$$\dot{m} \frac{dC_2}{dx} = W_I (C_1 - C_2) + 2W_{II} (C_4 - C_2)$$

$$\dot{m} \frac{dC_2}{dx} = W_{II} (C_1 - C_3)$$

$$\dot{m} \frac{dC_4}{dx} = W_{II} (C_2 - C_4)$$

where:

C_i = concentration of i th channel

W_I = turbulent interchange mixing coefficient between central subchannels

W_{II} = turbulent interchange mixing coefficient between a central and a peripheral channel

$\dot{m}$ = subchannel mass flowrate

W_{II} is not directly attainable since we cannot measure the output concentration of the peripheral channels. Instead, it is set as a multiple of W_I. A parametric study of its effect upon the determined value of W_I will be made, but an order of magnitude argument indicates that it shouldn't change W_I by more than 1-2%.

In the case where a diversion crossflow exists some additional assumptions must be made, most importantly that the majority of the crossflow is between the two central subchannels. Then the equations become:

$$\dot{m} \frac{dC_1}{dx} = (W_I + W_C)(C_2 - C_1) + 2W_{II}(C_3 - C_1)$$

$$\dot{m} \frac{dC_2}{dx} = (W_I - W_C)(C_1 - C_2) + 2W_{II}(C_4 - C_2)$$

$$\dot{m} \frac{dC_3}{dx} = W_{II}(C_1 - C_3)$$

$$\dot{m} \frac{dC_4}{dx} = W_{II}(C_2 - C_4)$$

where:

W_C = diversion crossflow

An additional set of these four equations must be added for the case where the traced channels are switched from right to left. Summarizing this system of equations, we have eight equations, all initial conditions (input concentrations) known, output concentrations for untraced central subchannel known, and 8 unknowns. The unknowns are:

a) Coefficients; W_I and W_C

b) Output concentrations (T represents traced, R represents untraced);

- C_{1T}, C_{2T}, C_{3T}, C_{4T}, and C_{3R}.

The computer program that iterates the solution of these equations until the correct values of W_I and W_C have been found has been written and is now being debugged.

Delivery of the Datametrics system should be in about a month. Mixing tests can begin again about the end of October. In the meantime, another pump and flowmeter have been added to increase our Reynold's number range from 25,000 to 50,000.

TASK IIC. Experimental Subchannel Local Parameter Measurements (Laser Doppler Anemometer)

No work was performed this quarter.

TASK IID. Analytic Model Development - Subchannel

No work was performed this quarter.

TASK III: LMFBR OUTLET PLENUM FLOW MIXING

TASK IIIA: Analytical and Experimental Investigation of Velocity and Temperature Fields (Y.B. Chen, Ralph Bennett)

In this task, which is concerned with the development of design methods for use in characterizing the flow distribution in the LMFBR outlet plenum, there are parallel analytical and experimental efforts. The experimental work is concerned with measurements of the turbulent velocity and temperature fields in the outlet plenum geometry, and the analytical work with determination of the best turbulence model for use in design calculations.

Experimental Effort: In the experimental work two parallel developments - concerned with velocity field measurements and with temperature measurements - have been carried on. In both cases the experiments are performed in a two-dimensional geometry which matches the transverse dimensions of the ANL 1/15-scale outlet plenum test cell (see Figs. III.1 and III.2). The two-dimensional cartesian geometry was chosen because the optical velocity and temperature measurement techniques are difficult to use when the light beams must penetrate a curved boundary, or when a thick flow section is used (as with a cylindrical drum). Thus, the experiments are performed in a thin cartesian-geometry section as shown. This also avoids the problems of azimuthal asymmetry in the flow field, which would be expected in the cylindrical geometry due to the use of discrete (although symmetrical) outlet nozzles.

III.1 Velocity Field Measurements (Y.B. Chen)

The velocity field experiment is in the final stage of preparation. The water flow loop and experimental cell are assembled and in place (shown in Fig. III.3). However, the LDA system became available to this experiment only in mid-September so no measurements have been made yet. In late August this system was modified by the purchase of a new optical unit, to facilitate the backscattering detection mode of the rod-bundle mixing experiment.

Unanticipated difficulties in de-bugging the modified experimental system have delayed initiation of the outlet plenum velocity measurement experiments. Consultations with the optical unit vendor are currently underway, in order to provide a resolution to the problem. Following this resolution the experiments will begin. This is expected to occur in mid-October.

III.2 Temperature Field Measurements (R. Bennett)

The temperature field measurement effort consists of a developmental program to provide a non-intrusive method for temperature measurements in turbulent flow. Such a method is needed in order to provide a temperature signal which reflects rapid changes in temperature due to eddy motion, and which does not require a mechanical probe which can disturb the fluid flow. The technique being used is that of a Mach-Zehnder interferometer. Experimental work has been under way since late April, and the results to-date are very promising. The fluid used in the experiments is air.

The Mach-Zehnder interferometer (shown in Fig. III.4) for non-intrusive temperature measurements in thin flows has been built. A laser illuminates the interferometer, and produces very good quality fringes for detection. An inexpensive semiconductor circuit satisfactorily detects the output intensity, with exceptionally fast time-response. The interferometer was aligned successfully with the model outlet-plenum plexiglas test cell inserted in one arm, so it follows that special optically flat windows in the test cell are not required - as had once been feared. In the laboratory space used initially troublesome low frequency vibrations from machinery in the building could not be eliminated, so the system has been moved to a basement location, where much better performance has been obtained.

The interferometer has been demonstrated successfully in experiments using air as the experimental fluid in the outlet plenum geometry. The early results are reported in Appendix III.1, the abstract of a paper accepted for presentation at the November, 1975 meeting of the American Nuclear Society in San Francisco, California. More recent results are shown in Figs. III.6 and III.7 in which the photodiode output voltage is displayed as a function of time. It is seen that in the first set of measurements that the observed turbulent temperature fluctuation is of the order of half the value of the temperature difference in the parallel inlet flow channels, and the time scale of the fluctuations is of the order of 25 msec. In the second set of measurements it is seen (Table III.1) that the temperature fluctuation amplitude is about 15% of the inlet flow temperature difference, and the fluctuation time-scale is about 5 msec. In the two sets of measurements shown, temperature data were obtained simultaneously using the Mach-Zehnder interferometer and the 28-gauge chromel-alumel thermocouple positioned as shown in Fig. III.5. It is seen that in each case the sensor locations were symmetrically opposite each other, above the inlet flow divider plates. However, in the first set of measurements the

thermocouple wire entered the test cell at the nearest outlet plenum, and caused significant flow disruption. In the second set of measurements it entered the test cell through a tiny hole in the cell wall adjacent to the point of measurements, thereby greatly reducing the flow disruption. In each case the ability of the Mach-Zehnder interferometer to observe rapid temperature fluctuations is clearly demonstrated. It is notable also that in each case the thermocouple was almost totally insensitive to these fluctuations - despite the small size of the probe (28-gauge wire, each of 0.0156 in. diameter, and junction response time estimated to be $\approx$ 25 msec).

In the next stage of work the detecting system will be improved to reduce background noise; and velocity and temperature correlation work will be started.

III.3 Analytical Effort (Y.B. Chen)

During the past quarter the two-dimensional, incompressible, two-equation turbulence model code TEACH[1] has been made operational on the Laboratory for Nuclear Sciences (LNS) IBM-360 (65). It is being used to analyze the outlet-plenum scale model experiments being performed in this program, and it is the vehicle for testing the various proposed turbulence models. It has been used to calculate the expected flow distribution in the outlet plenum 1/15-scale test section, as well as the associated eddy momentum diffusivity, and turbulence kinetic energy fields (examples of these results are shown in Fig. III.8, and Tables III.2 and III.3, respectively).

Due to difficulties encountered in trying to use the code VARR-II[2] (to be used in transient two-dimensional incompressible, recirculating flow calculations) on either of the IBM computers at MIT a new direction has been undertaken in getting the code operational. Through the LNS computer facility the program is being transmitted to the ERDA-owned CDC-6600 computer at the University of California, Berkeley, using the DOD Advanced Research Projects Agency (ARPA) network. This is being done because VARR-II is not written entirely in FORTRAN, but has some machine-language subroutines which take advantage of CDC system features. This has made it very difficult to use on an IBM system, and has required use of a remote computer. Due to the difficulties in transmission the code has not yet been run successfully on the Berkeley machine.

References

1. A.D. Gosman, Listing of the TEACH-T Computer Program and Sample Output, Penn. State Univ. (1975).

2. J.L. Cook and P.I. Nakayama, VARR-II Computer Program for Calculating Time Dependent Turbulent Fluid Flows with Slight Density Variation, WARD-D-0106, Westinghouse Electric Co. (1975).

TABLE III.1

Temperature Fluctuation Measurement Cases

Run No.	Temp. in Hot Leg (°F)	<T> (°F)	Hot Inlet Flow (ft/sec)	Hot Inlet Re μ = const.	Maximum ΔT Possible (°F)	(Estimated) T' Range (°F)	(Estimated) Duration (msec)	2(Avg-Low) (°F)
Set 1								
1	71	71	0	---	---	Noise, 6°	---	---
2	71	71	3.33	180	---	Noise, 10°	---	---
3	125	80.3	3.67	194	54°	21°	10,25,50	19° *
4	150	86.0	3.83	201	79°	32°	10,25-50	30° *
5	140	88.5	3.33	174	69°	33°	25-50	35° *
6	165	99.3	3.83	196	94°	56°	25-50	57°
7	160	99.8	3.83	196	89°	25°	25-50	58°
8	160	98.0	3.83	197	89°	40°	25-75	54°
9	165	99.1	3.83	196	94°	53°	25-75	56° *
10	135	96.2	0	Convection	64°†	60°	500-2,000	50° *
11	115	95.1	0	Convection	44°†	46°	500-1,200	48° *
12	105	83.7	3.67	193	34°	19°	25-125	25° *
Set 2								
13	68	71	4.00	216	---	Noise, 6°	---	---
14	70	71	0	---	---	Noise, 3°	---	---
15	90	78.6	4.08	217	20°	20°	≈ 5	17°
16	130	97.7	4.33	222	60°	16°	∿ 5	35°
17	150	110.4	4.50	226	80°	18°	∿ 5	80°
18	172	114.2	4.50	224	102°	15°	2-4	88°
19	NR	117.0	4.50	223	NA	18°	∿ 5	94°
20	150	118.4	4.67	231	80°	15°	∿ 5	97°
21	155	118.0	4.67	231	85°	13°	2-8	96°
22	175	117.7	4.33	215	105°	15°	1-6	96°
23	175	119.0	4.83	239	105°	14°	1-6	98°
24	160	122.4	4.67	229	90°	14°	2-6	105°

*Total ΔT ≈ 2(Avg-Low) within 10°

†Total ΔT ≈ High-Low within 10°

TABLE III.2

Teach Calculation, 1/15-Scale Test, Re = 50,000

TURBULENT VISCOSITY

I=		2	3	4	5	6	7	8	9	10
X=		0.006	0.019	0.032	0.044	0.057	0.070	0.083	0.095	0.108
	Y=									
J										
14	0.159	8.00E-04	8.00E-04	8.00E-04	8.00E-04	8.00E-04	8.00E-04	8.00E-04	8.00E-04	8.00E-04
13	0.146	1.64E-02	1.44E-01	6.81E-02	1.76E-02	1.61E-02	1.63E-02	1.66E-02	1.69E-02	1.71E-02
12	0.133	2.06E-02	2.01E-01	1.73E-01	1.18E-01	9.73E-02	9.32E-02	9.28E-02	9.31E-02	9.36E-02
11	0.121	1.94E-02	1.91E-01	1.89E-01	1.55E-01	1.43E-01	1.40E-01	1.39E-01	1.37E-01	1.34E-01
10	0.108	1.78E-02	1.79E-01	1.94E-01	1.86E-01	1.76E-01	1.77E-01	1.77E-01	1.75E-01	1.70E-01
9	0.095	1.62E-02	1.66E-01	1.92E-01	1.99E-01	1.99E-01	2.03E-01	2.07E-01	2.07E-01	2.03E-01
8	0.083	1.47E-02	1.48E-01	1.84E-01	2.01E-01	2.11E-01	2.19E-01	2.25E-01	2.28E-01	2.26E-01
7	0.070	1.32E-02	1.29E-01	1.72E-01	1.96E-01	2.12E-01	2.24E-01	2.32E-01	2.37E-01	2.36E-01
6	0.057	1.17E-02	1.11E-01	1.56E-01	1.84E-01	2.04E-01	2.18E-01	2.26E-01	2.30E-01	2.29E-01
5	0.044	1.03E-02	9.38E-02	1.37E-01	1.66E-01	1.83E-01	1.93E-01	1.97E-01	1.99E-01	1.98E-01
4	0.032	9.30E-03	7.64E-02	1.13E-01	1.24E-01	1.29E-01	1.33E-01	1.37E-01	1.41E-01	1.44E-01
3	0.019	2.04E-02	4.09E-02	5.68E-02	6.96E-02	8.00E-02	8.86E-02	9.59E-02	1.02E-01	1.07E-01
2	0.006	2.28E-03	2.43E-03	2.73E-03	3.26E-03	4.12E-03	5.41E-03	7.19E-03	9.49E-03	1.23E-02

TABLE III.2 (continued)

Teach Calculation, 1/15-Scale Test, Re = 50,000

TURBULENT VISCOSITY

I=		11	12	13	14	15	16	17	18	19	20
X=		0.121	0.133	0.146	0.159	0.171	0.184	0.197	0.210	0.222	0.235
	Y=										
J											
14	0.159	8.00E-04	8.00E-04	8.00E-04	8.00E-04	8.00E-04	8.00E-04	8.00E-04	8.00E-04	8.00E-04	8.00E-04
13	0.146	1.72E-02	1.73E-02	1.73E-02	1.73E-02	1.73E-02	1.73E-02	1.74E-02	1.74E-02	1.64E-02	8.00E-04
12	0.133	9.41E-02	9.45E-02	9.47E-02	9.44E-02	9.31E-02	8.93E-02	7.92E-02	5.98E-02	1.65E-02	8.00E-04
11	0.121	1.30E-01	1.25E-01	1.21E-01	1.17E-01	1.12E-01	1.06E-01	9.56E-02	7.29E-02	1.65E-02	8.00E-04
10	0.108	1.63E-01	1.53E-01	1.43E-01	1.33E-01	1.24E-01	1.16E-01	1.06E-01	8.21E-02	1.72E-02	8.00E-04
9	0.095	1.95E-01	1.83E-01	1.67E-01	1.50E-01	1.36E-01	1.24E-01	1.12E-01	8.89E-02	1.80E-02	8.00E-04
8	0.083	2.18E-01	2.05E-01	1.88E-01	1.68E-01	1.48E-01	1.31E-01	1.17E-01	9.46E-02	1.88E-02	8.00E-04
7	0.070	2.29E-01	2.16E-01	1.98E-01	1.78E-01	1.57E-01	1.37E-01	1.21E-01	9.92E-02	1.94E-02	8.00E-04
6	0.057	2.22E-01	2.11E-01	1.95E-01	1.76E-01	1.57E-01	1.38E-01	1.28E-01	1.02E-01	2.01E-02	8.00E-04
5	0.044	1.93E-01	1.85E-01	1.75E-01	1.62E-01	1.48E-01	1.34E-01	1.20E-01	1.02E-01	2.10E-02	8.00E-04
4	0.032	1.45E-01	1.45E-01	1.43E-01	1.39E-01	1.32E-01	1.24E-01	1.12E-01	9.75E-02	2.27E-02	8.00E-04
3	0.019	1.11E-01	1.13E-01	1.14E-01	1.13E-01	1.10E-01	1.04E-01	9.38E-02	8.25E-02	2.62E-02	8.00E-04
2	0.006	1.54E-02	1.87E-02	2.19E-02	2.48E-02	2.70E-02	2.77E-02	3.04E-02	4.04E-02	3.50E-02	8.00E-04

TABLE III.3

Teach Calculation, 1/15-Scale Test, Re = 50,000

TURBULENÇE KINETIC ENERGY

I=		2	3	4	5	6	7	8	9	10
X=		0.006	0.019	0.032	0.044	0.057	0.070	0.083	0.095	0.108
	Y=									
J										
14	0.159	0.0	4.69E-04	4.69E-04	0.0	0.0	0.0	0.0	0.0	0.0
13	0.146	1.15E-04	1.58E-03	5.67E-04	1.33E-04	1.11E-04	1.14E-04	1.18E-04	1.22E-04	1.25E-04
12	0.133	1.84E-04	1.16E-04	7.40E-04	4.65E-04	3.43E-04	3.24E-04	3.23E-04	3.28E-04	3.34E-04
11	0.121	1.63E-04	9.15E-04	7.40E-04	4.98E-04	4.28E-04	4.12E-04	4.06E-04	4.01E-04	3.94E-04
10	0.108	1.36E-04	7.33E-04	6.50E-04	5.19E-04	4.73E-04	4.65E-04	4.61E-04	4.53E-04	4.38E-04
9	0.095	1.12E-04	5.90E-04	5.70E-04	5.10E-04	4.89E-04	4.92E-04	4.96E-04	4.93E-04	4.79E-04
8	0.083	9.04E-05	4.70E-04	4.97E-04	4.82E-04	4.82E-04	4.96E-04	5.09E-04	5.15E-04	5.10E-04
7	0.070	7.22E-05	3.76E-04	4.30E-04	4.46E-04	4.62E-04	4.84E-04	5.06E-04	5.21E-04	5.26E-04
6	0.057	5.65E-05	3.04E-04	3.71E-04	4.06E-04	4.34E-04	4.63E-04	4.92E-04	5.16E-04	5.32E-04
5	0.044	4.25E-05	2.48E-04	3.23E-04	3.71E-04	4.10E-04	4.47E-04	4.82E-04	5.15E-04	5.42E-04
4	0.032	3.41E-05	2.08E-04	3.07E-04	3.76E-04	4.31E-04	4.78E-04	5.21E-04	5.60E-04	5.93E-04
3	0.019	1.80E-04	4.14E-04	5.45E-04	6.31E-04	6.89E-04	7.30E-04	7.57E-04	7.75E-04	7.85E-04
2	0.006	2.39E-04	1.53E-04	1.16E-04	1.00E-04	9.55E-04	9.76E-05	1.04E-04	1.18E-04	1.24E-04

TABLE III.3 (continued)

Teach Calculation, 1/15-Scale Test, Re = 50,000

TURBULENCE KINETIC ENERGY

I=		11	12	13	14	15	16	17	18	19	20
X=		0.121	0.133	0.146	0.159	0.171	0.184	0.197	0.210	0.222	0.235
	Y=										
J											
14	0.159	0.0	0.0	0.0	0.0	0.0	0.0	0.0	0.0	0.0	0.0
13	0.146	1.28E-04	1.29E-04	1.29E-04	1.29E-04	1.28E-04	1.28E-04	1.30E-04	1.30E-04	1.15E-04	0.0
12	0.133	3.41E-04	3.50E-04	3.61E-04	3.73E-04	3.85E-04	3.92E-04	3.80E-04	3.22E-04	1.17E-04	0.0
11	0.121	3.88E-04	3.83E-04	3.81E-04	3.84E-04	3.92E-04	4.03E-04	4.04E-04	3.56E-04	1.16E-04	0.0
10	0.108	4.18E-04	3.98E-04	3.81E-04	3.73E-04	3.80E-04	3.99E-04	4.18E-04	3.87E-04	1.26E-04	0.0
9	0.095	4.56E-04	4.26E-04	3.97E-04	3.79E-04	3.80E-04	4.03E-04	4.33E-04	4.16E-04	1.39E-04	0.0
8	0.083	4.92E-04	4.64E-04	4.33E-04	4.09E-04	4.02E-04	4.21E-04	4.53E-04	4.46E-04	1.52E-04	0.0
7	0.070	5.19E-04	5.00E-04	4.75E-04	4.52E-04	4.41E-04	4.52E-04	4.80E-04	4.78E-04	1.63E-04	0.0
6	0.057	5.38E-04	5.33E-04	5.19E-04	5.02E-04	4.91E-04	4.95E-04	5.12E-04	5.10E-04	1.75E-04	0.0
5	0.044	5.61E-04	5.70E-04	5.70E-04	5.63E-04	5.54E-04	5.48E-04	5.46E-04	5.38E-04	1.93E-04	0.0
4	0.032	6.20E-04	6.38E-04	6.46E-04	6.45E-04	6.33E-04	6.12E-04	5.75E-04	5.52E-04	2.27E-04	0.0
3	0.019	7.88E-04	7.82E-04	7.66E-04	7.40E-04	7.00E-04	6.42E-04	5.60E-04	5.18E-04	3.04E-04	0.0
2	0.006	1.35E-04	1.45E-04	1.54E-04	1.60E-04	1.61E-04	1.59E-04	1.75E-04	2.76E-04	5.51E-04	0.0

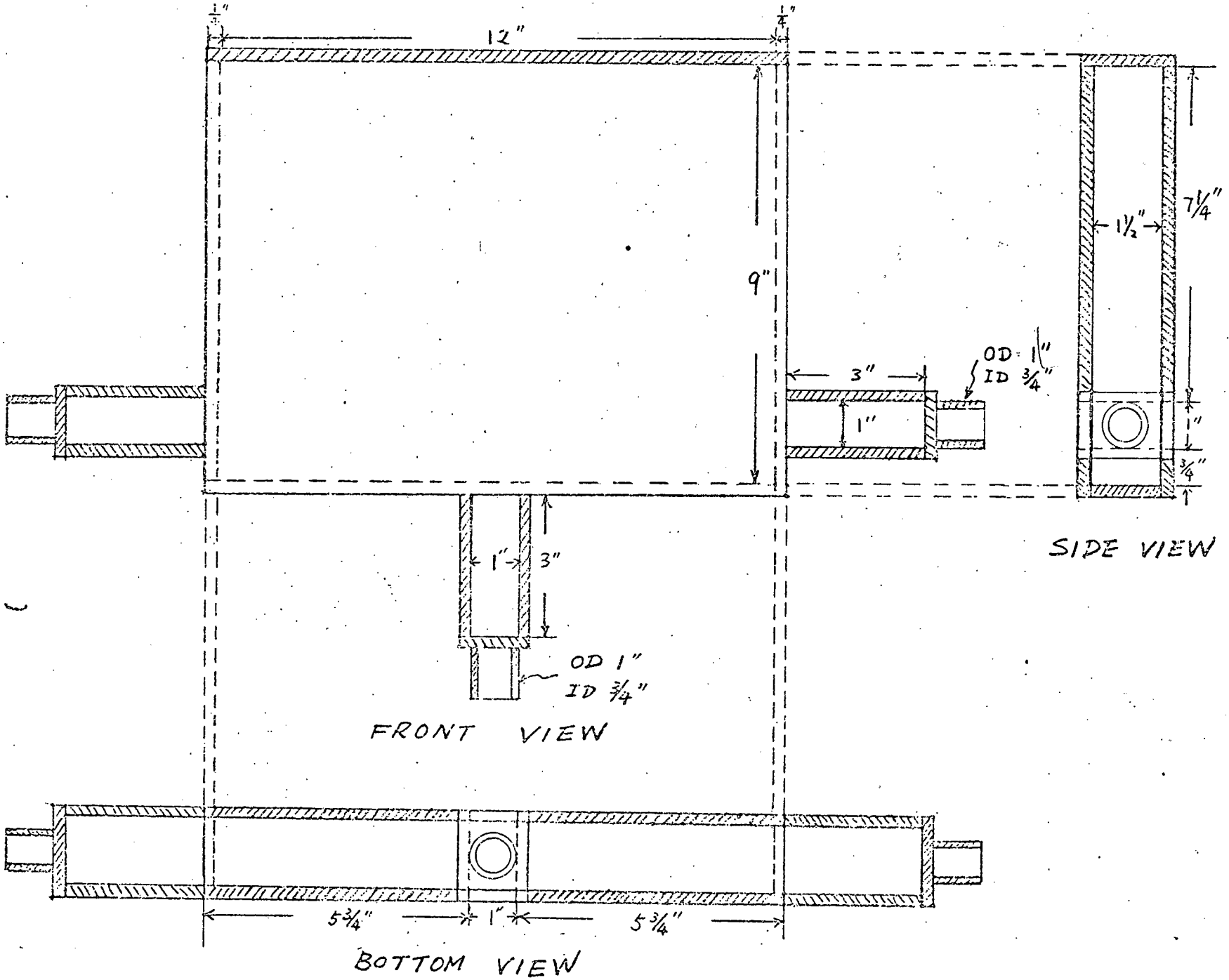

FIG. III.1: Velocity Measurement Test Section

FIG. III.2: Velocity Measurement Flow Schematic

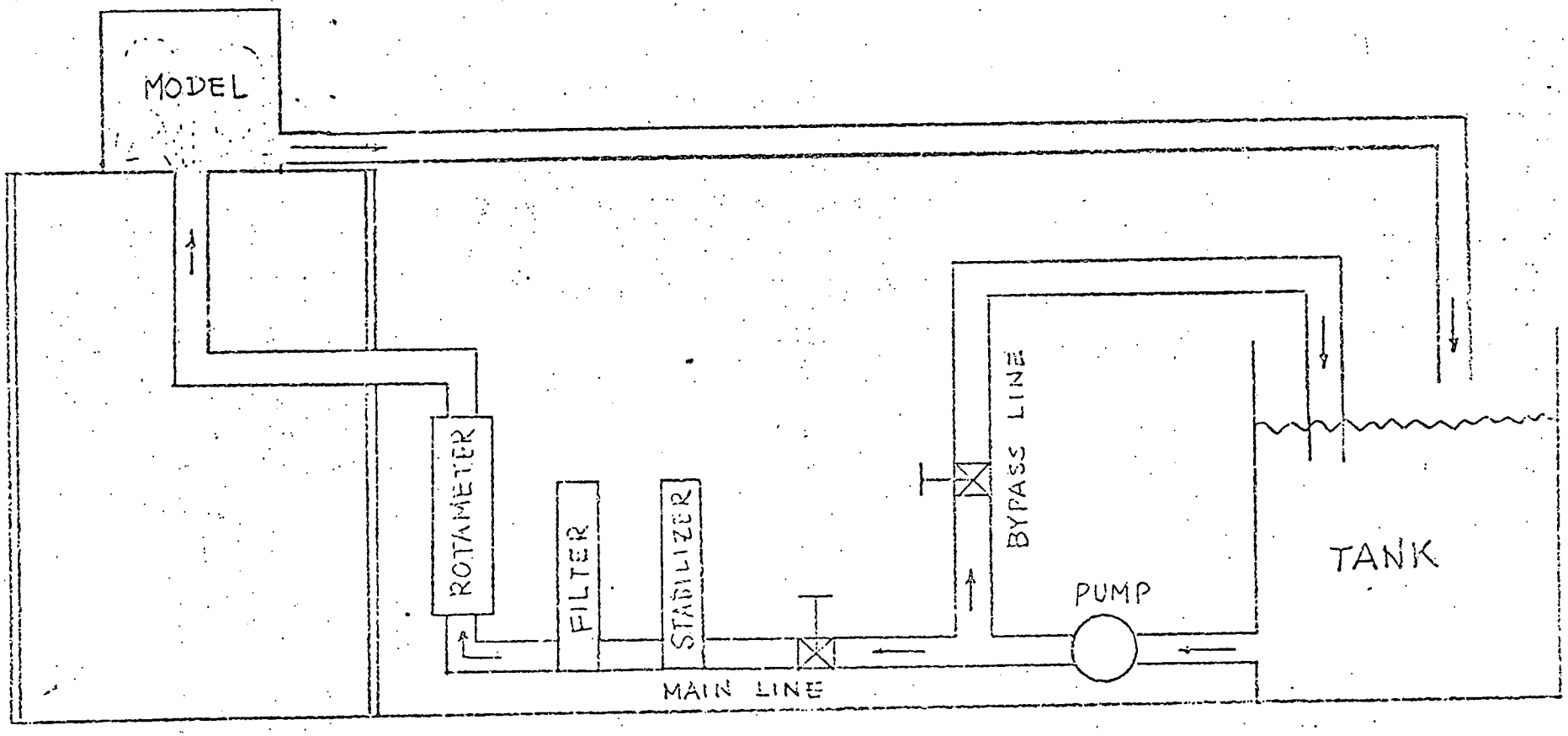

SCHEMATIC FLOW DIAGRAM

FIG. III.3: Velocity Measurement Detection System

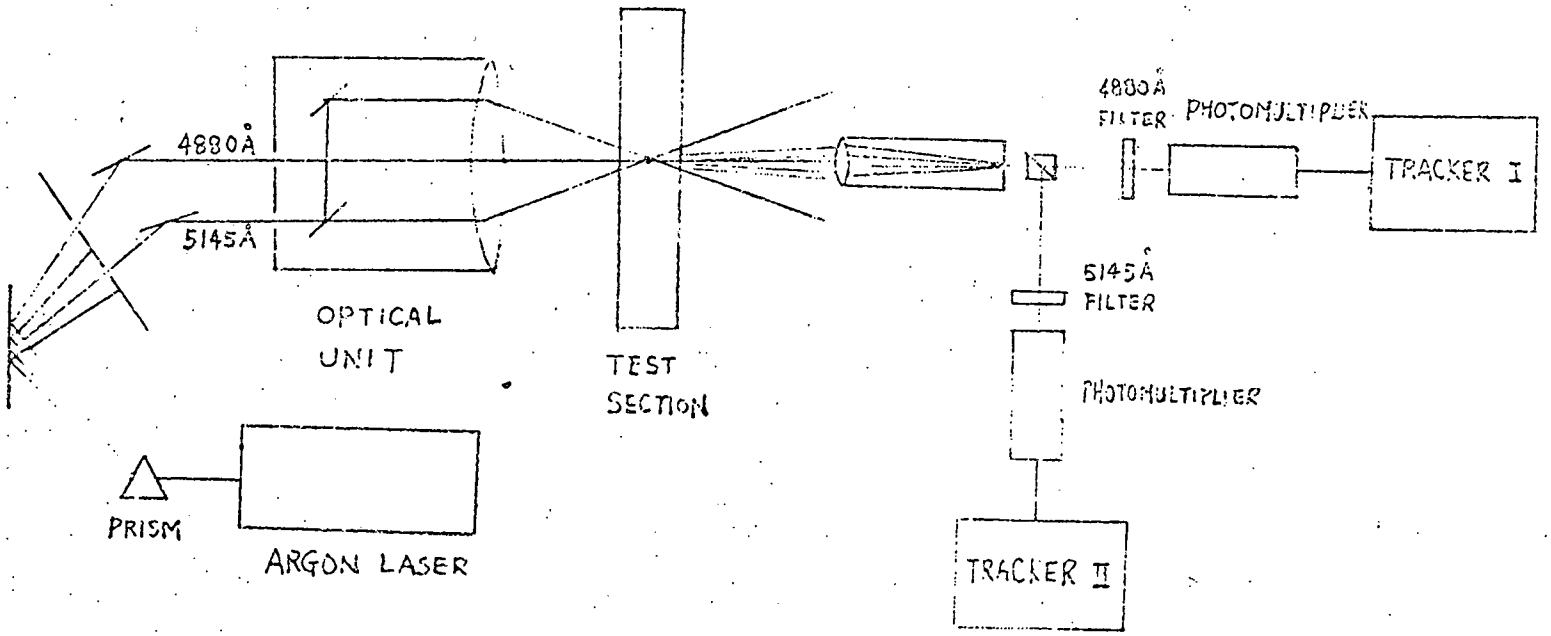

SCHEMATIC DIAGRAM OF LDA SETUP

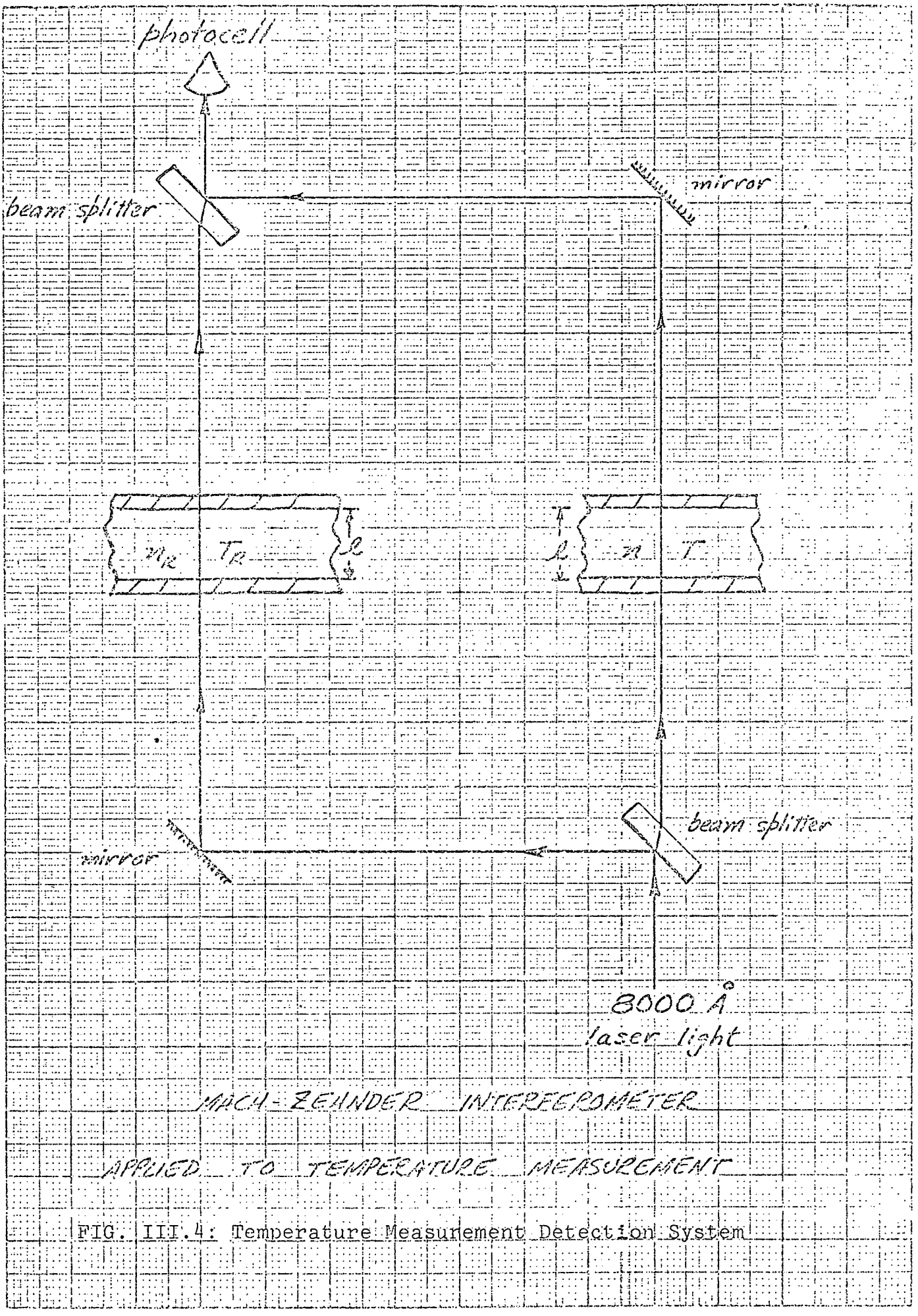

FIG. III.4: Temperature Measurement Detection System

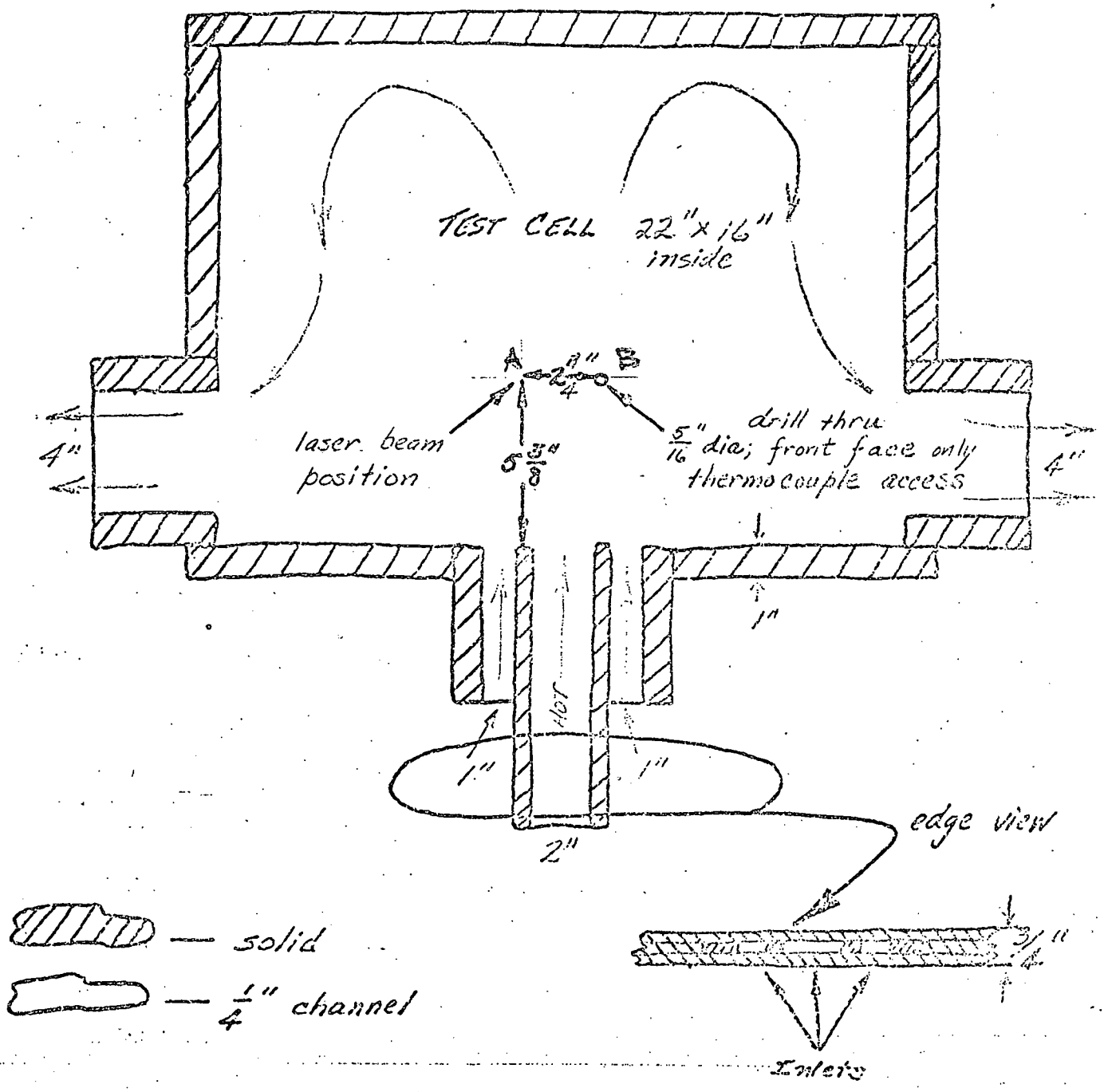

FIG. III.5: Points of Turbulent Temperature Measurement,
Point A = Interfermoeter Measurement Station,
Point B = Thermocouple Measurement Station

FIG. III.6: Sample Interferometer Temperature Measurements Set 1,

a) Run No. 1, Background Noise (building Vibrations) with Heater Off, Blower On,

b) Run No. 8, Hot Leg Temperature 160°F, = 3.8 fps Inlet

For Both Runs:

Horizontal Scale = 100 msec/division

Vertical Scale = 25 °F/division, both runs

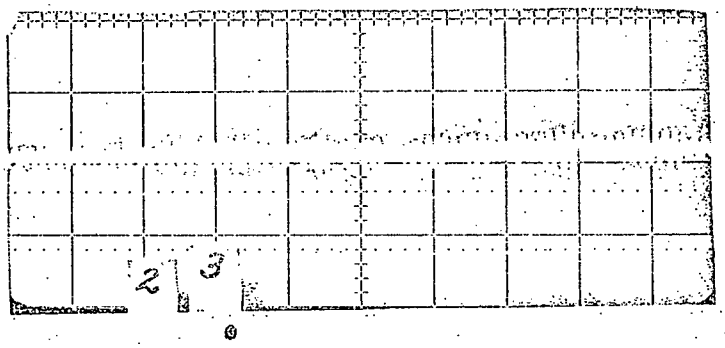
2
3

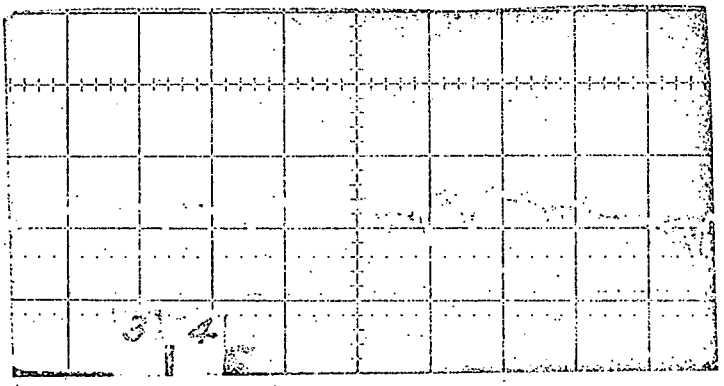
3
4

FIG. III.7: Sample Interferometer Temperature Measurements, Set 2

a) Run No. 13, Background Noise (Building Vibrations) with Heater Off, Blower On, Horizontal Scale = 50 msec/division

b) Run No. 23, Hot Leg Temperature = 175 °F
Inlet = 4.8 fps.
Horizontal Scale = 10 msec/division
Vertical Scale = 25 °F/division, both runs

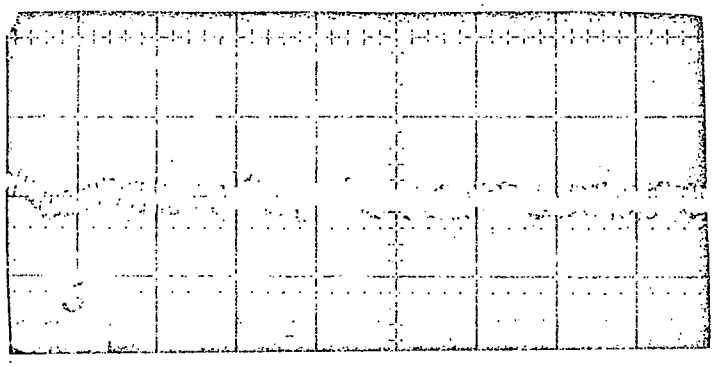

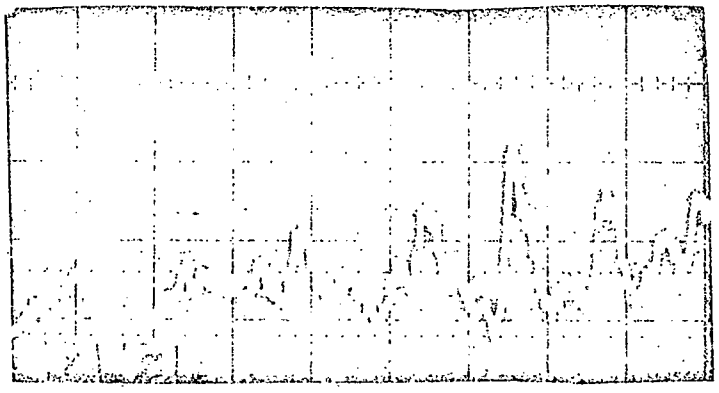

FIG. III.8: Velocity Field Calculated by TEACH, 1/15-Scale Test, Re = 50,000

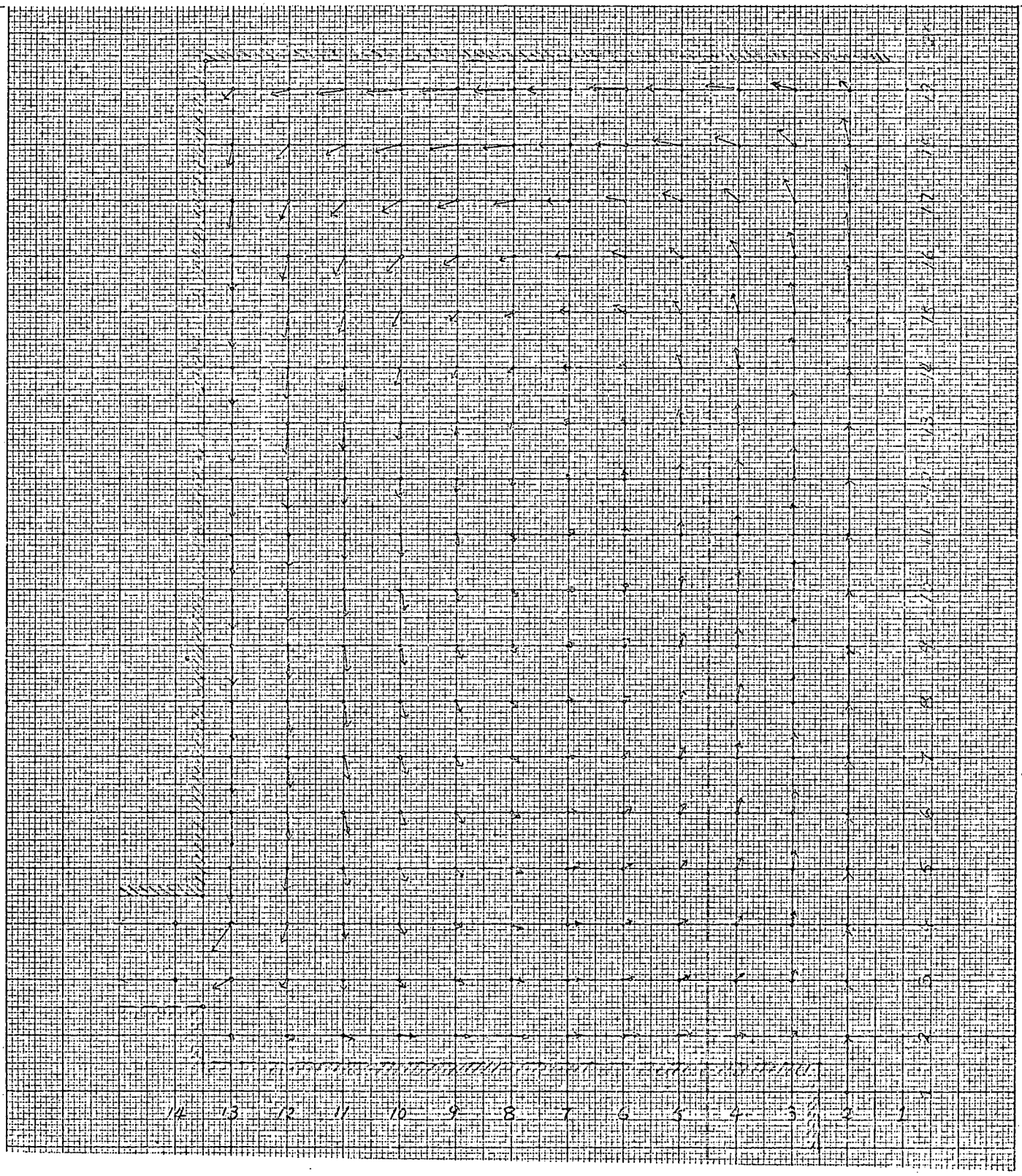

Velocity Distribution Predicted by TEACH